Membrane Protein Structure

DOI: 10.1002/anie.201100730

The Conformation of Bacteriorhodopsin Loops in Purple Membranes Resolved by Solid-State MAS NMR Spectroscopy**

*Victoria A. Higman, Krisztina Varga, Lubica Aslimovska, Peter J. Judge, Lindsay J. Sperling, Chad M. Rienstra, and Anthony Watts**

Membrane proteins (and rhodopsin-like G-protein coupled receptors (GPCRs), in particular) are of significant biological and medical importance since they represent over 50% (GPCRs 25%) of current drug targets.[1] However, the structure determination of membrane proteins is challenging: currently they account for <1% of the unique protein structures deposited in the Protein Databank.[2] X-ray crystallography has been used to make major contributions towards the structure determination of membrane proteins,[3] but it suffers from the fact that the proteins are rarely crystallized in their native lipid environment or are unmodified, and exposed loop regions are often either dynamic and not visible, or involved in crystal contacts. NMR spectroscopic studies of membrane proteins in solution are generally also reliant on an artificial detergent environment and are also limited by protein size. Solid-state NMR (ssNMR) spectroscopy, in contrast, has the advantage that membrane proteins can be studied in a lipid environment.[4] Although ssNMR does not suffer from the same intrinsic size limitation as solution NMR spectroscopy, spectral overlap is often severe for large proteins and hampers their study. However, magic-angle-spinning (MAS) NMR spectroscopy, in particular, has been used to make substantial methodological advances in recent years, and the first membrane protein structures have now been determined using this technique.[5]

Herein we report on how solid-state MAS NMR spectroscopy can be used to complement X-ray crystallographic studies of a large seven transmembrane (7TM) helical protein by validating and redefining the loop structures. The structure of bacteriorhodopsin (bR) has been determined in a range of two- (2D) and three-dimensional (3D) crystalline environments with the loops showing the highest degree of structural variation.[6] Solid-state MAS NMR spectra of uniformly [^{13}C,^{15}N]-labeled bR in its native purple membrane have been used to assign the signals of the loop regions of the protein. Extraction of dihedral angle information from chemical shifts has allowed us to validate several loop conformations in the crystal structure and recalculate the structure where there are differences in conformation.

Ab initio assignment of the resonances of the loop regions of bR was carried out using 2D DARR spectra (mixing times of 15 and 50 ms) and 3D NCACX (20 ms), 3D NCOCX (20 ms), 3D CANCO and 3D CAN(CO)CX (45 ms) spectra. Assignment of the loops is made possible by the fact that the loop resonances are generally well separated and amenable to assignment in contrast to many of the helical regions, where leucine and valine resonances, in particular, exhibit intractable degrees of spectral overlap. Figure 1 shows the assignment of the section Met68–Gly72 in the BC loop as an example; further 2D spectra and strip plots are provided in the Supporting Information (Figures S1–S3). In total, we have assigned roughly 55% of loop residues covering all loops, except for the CD loop, as well as several residues located in the helices (Figure 2, Table S2 in the Supporting Information, and BMRB Accession code 17361). Interestingly, residues from all loops (except those in the unassigned CD loop) are visible in our cross-polarization (CP)-based spectra; this is in contrast to the spectra of sensory rhodopsin II from *Natronomonas pharaonis* (NpSRII) where most loops were visible only in INEPT-based spectra,[7] reflecting a higher degree of loop mobility in NpSRII. Our observations are more similar to those made in a recent study of proteorhodopsin in which only isolated residues were observed in INEPT-based spectra.[8] A ^{13}C,^{13}C INEPT-COSY spectrum of bR contains resonances with random-coil chemical shifts from amino acid types that are consistent with the N- and C-terminal tails (see Figures S4 and S5 in Supporting Information). Some chemical shifts for side chains in non-random-coil conformations are also found for residues Lys, Glu, Ala, and Ser, which may belong to the KAES motif in the EF loop. Sequential

[*] Dr. V. A. Higman,[+] Dr. P. J. Judge, Prof. A. Watts
Department of Biochemistry, University of Oxford
South Parks Road, Oxford, OX1 3QU (UK)
E-mail: anthony.watts@bioch.ox.ac.uk
Dr. K. Varga[+]
Department of Chemistry, University of Wyoming
Laramie, WY 82071 (USA)
Dr. L. Aslimovska
Institut für Biophysikalische Chemie, Goethe-Universität
60438 Frankfurt (Germany)
L. J. Sperling, Prof. C. M. Rienstra
Department of Chemistry
University of Illinois at Urbana-Champaign
Urbana, IL 61801 (USA)
[+] These authors contributed equally to this work.

[**] We acknowledge financial support from EPSRC (grants GR/R99393/01 and EP/C015452/1), Bionanotechnology IRC, Magnex Scientific and Varian Inc., NIH (R01GM075937 to C.M.R. and Molecular Biophysics Training Grant PHS 5 T32 GM008276), bridging support from the University of Oxford (to V.A.H.), and a Ullyot Fellowship (to L.J.S.). This work has benefited from the activities of the DLAB & JRA7 consortia funded by the EU under contracts HPRI-2001-50065 and RII3-CT-2003-505925. We also thank the staff of the ILL-EMBL Deuteration Laboratory for advice as well as Ming Tang and the staff at the University of Illinois at Urbana-Champaign, School of Chemical Sciences NMR Facility for their technical support.
MAS = magic angle spinning.

Supporting information for this article is available on the WWW under http://dx.doi.org/10.1002/anie.201100730.

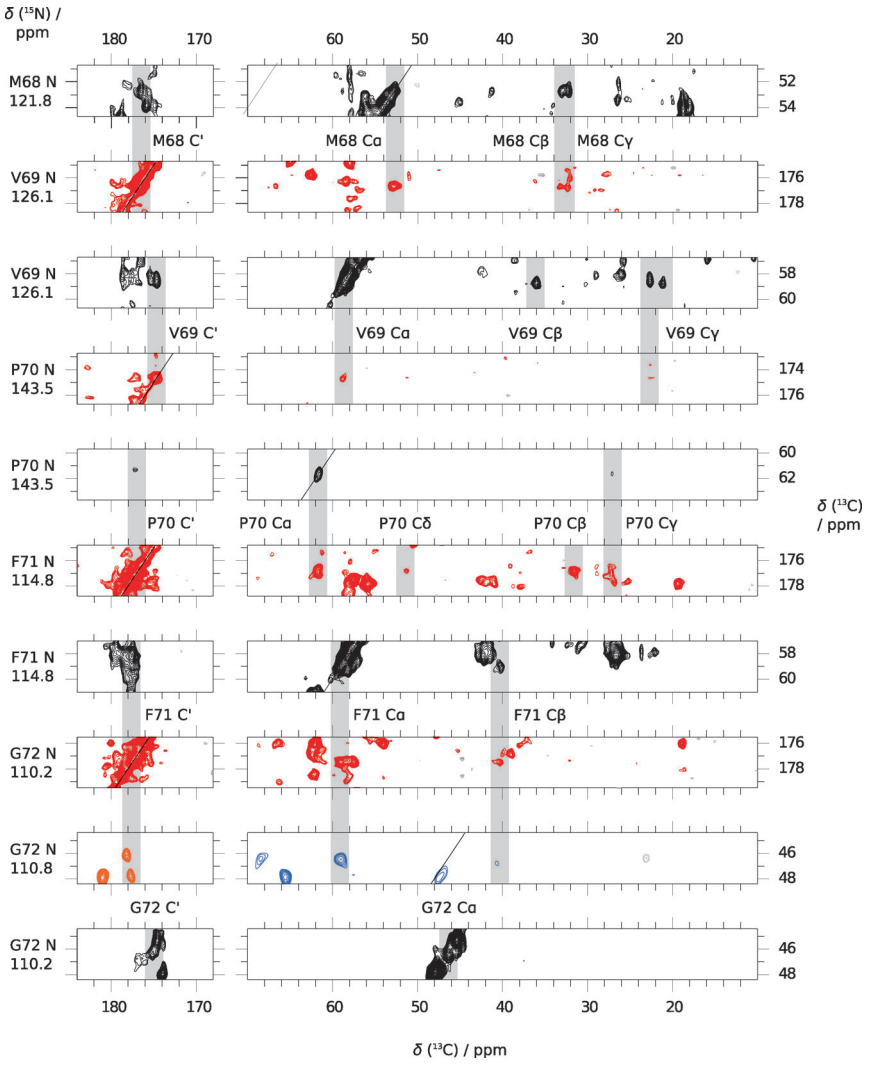

Figure 1. Assignment of Met68–Gly72 using NCACX (black, 20 ms mixing), NCOCX (red, 20 ms), CANCO (orange), and CAN(CO)CX (blue, 45 ms) spectra.

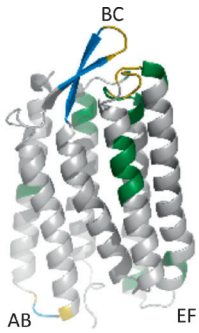

Figure 2. Ribbon representation of the 1QHJ crystal structure of bR showing residues that have been assigned and the dihedral angles predicted by TALOS+: α-helical (green), β-sheet (blue), and ambiguous (yellow).

assignment has so far not been possible. The number of signals in the INEPT spectra does not increase with temperature, suggesting that the loops in bR are relatively rigid.

Using the TALOS+ software,[9] we calculated dihedral ϕ and ψ angles for bR from the assigned chemical shifts. Figure 2 maps the residue assignments and predicted secondary structure onto the 1QHJ crystal structure, a high-resolution structure representative of many other high-quality crystal structures. Overall, good agreement is found between the secondary structure in the crystal and that from our NMR data recorded in the purple membrane. Comparisons can also be made with chemical shifts determined for some loop regions of bR solubilized in dodecyl maltoside with a deuterated dodecyl moiety (dDM) using solution NMR spectrscopy (Figure S6 in the Supporting Information).[10] In the AB loop we have assigned four out of seven residues and the chemical shifts are in good agreement with the shifts in solution. However, the TALOS+ predictions for Ser35 favor the extended/β-sheet region of the Ramachandran map, while the crystal structure favors the helical region. The β sheet observed in the BC loop in the crystal structure is also resolved in bR in the purple-membrane environment, where we have assigned 12 out of 18 residues. Few solution NMR assignments are available for this loop, which may be because the β sheet prevents ^{1}H–^{2}H exchange. The CD loop is very short and unfortunately it was not possible to obtain unambiguous assignments using the solid-state data. We assigned three of four residues in the short DE loop and the TALOS+ angles are in good agreement with the crystal structures, but no solution NMR data is available. The EF loop assumes various different conformations in the available bR crystal structures. In some crystal forms it is involved in crystal contacts, and in several structures residues 157–161 are not visible. However, the assignment of Phe156–Ser158 shows that these residues adopt a helical structure and are not significantly mobile. At least two conformations were observed for residues 153–159 in solution, and the Cα/Cβ/C′ shifts differ by several ppm from the solid-state chemical shifts. The EF loop clearly has the capacity for mobility under certain conditions but may be more rigid in the purple-membrane environment studied with solid-state NMR. Because of a lack of assignments, we cannot at this time confirm whether residues 159–164 may show some mobility even in the solid state. The dihedral angles predicted by TALOS+ for the seven out of nine assigned residues in the FG loop are in good agreement with the angles observed in the crystal structures. Comparison with solution NMR shifts is not possible for this stretch of residues.

The structure of the AB loop was recalculated based on the ϕ and ψ angles predicted by TALOS+ for Ser35 and Asp36. This results in a switch of the Ser35 dihedral angles

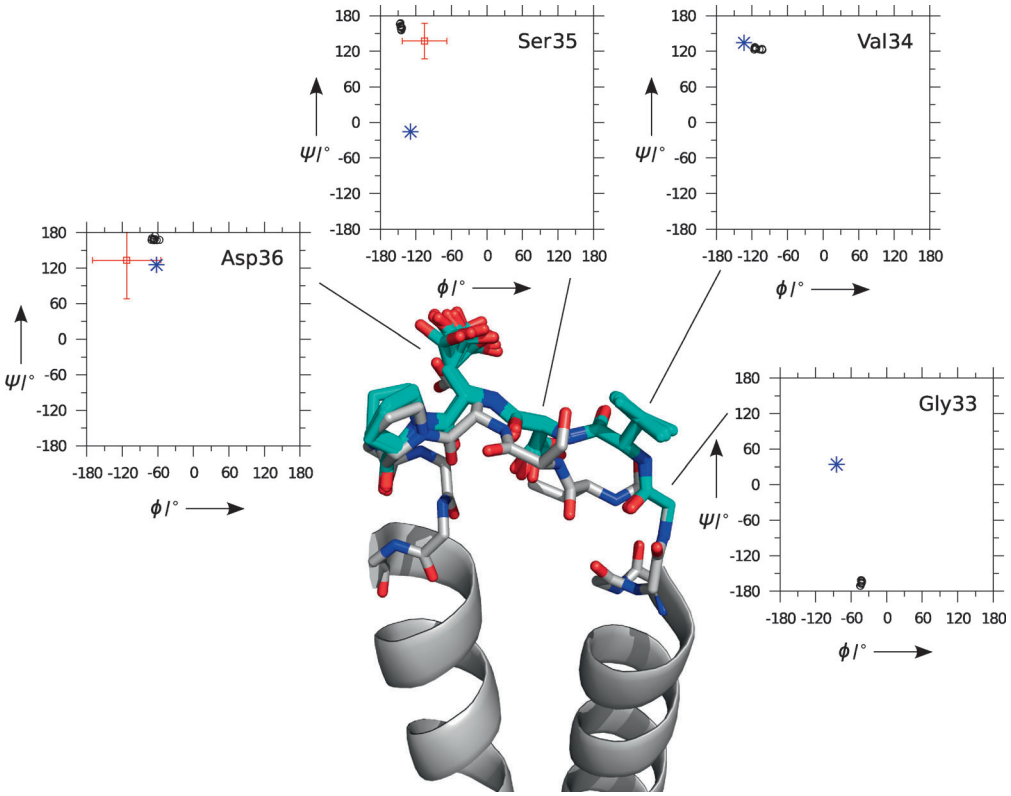

Figure 3. The AB loop of bR; the 1QHJ crystal structure is shown in gray, the 10 lowest-energy structures calculated using XPLOR based on the dihedral angles predicted by TALOS+ are shown in cyan. Side-chain conformations and Ramachandran plots are shown for Gly33–Pro37: 1QHJ crystal structure (blue stars), TALOS+ prediction (red squares), ensemble structure calculated by XPLOR-NIH (black circles).

which is compensated by a change in the Gly33 ϕ and ψ angles (Figure 3 and Figure S8 in the Supporting Information). Although these differences are unlikely to be relevant for the function of bR, they illustrate that differences in conformation between a membrane protein in crystal and native lipid environments can be observed and that refinement using solid-state NMR data is possible. A recent comparison of the influenza virus A M2 proton channel studied by X-ray crystallography as well as solution and solid-state NMR spectroscopy has highlighted the importance of either studying membrane proteins in their native lipid surroundings, or validating structures determined in other environments.[11]

Here we have shown how solid-state MAS NMR data collected on a large 7TM protein in its native membrane can be used to complement and verify the structure of (possibly distorted) loops in X-ray crystal structures, or solution NMR data obtained in alternative environments. Where the chemical shifts point towards conformational differences, an alternative loop structure in agreement with the ssNMR data can be calculated. Furthermore, while the resolution of new GPCR crystal structures has been achieved only by using thermostabilized mutants, complexes with antibody fragments, and constructs in which additional proteins had been inserted into a loop to promote crystallization,[12] our approach can provide important information about the native loop structures in wild-type proteins, in the presence and absence of both small-molecule ligands and proteins involved in signaling pathways.

Experimental Section

NMR samples were prepared as described previously.[13] 2D DARR,[14] and 3D NCACX, and 3D NCOCX NMR spectra[15] were recorded on an 800 MHz (^{1}H frequency) Varian/Magnex Infinity Plus NMR spectrometer equipped with a 3.2 mm HCN Balun probe with 10.776 kHz (DARR) or 10.0 kHz (NCACX, NCOCX) magic-angle-spinning and a variable temperature set point of −10 °C. 3D CANCO and 3D CAN(CO)CX spectra (45 ms DARR mixing)[16] were acquired on a 500 MHz (^{1}H frequency) Varian Infinity Plus spectrometer equipped with a 3.2 mm HCN Balun probe (with 11.111 kHz magic-angle spinning and a variable temperature set point of −25 °C). Data were processed using NMRPipe[17] and analyzed using CCPNmr Analysis.[18] Further details of data acquisition and processing can be found in the Supporting Information.

Structure calculations were conducted using XPLOR-NIH.[19] The 1QHJ crystal structure[20] was used as a starting structure, and all atoms were held fixed except for those in the AB loop. In addition to the dihedral angle restraints derived from TALOS+,[9] torsion angle restraints were used.[21] Further details are provided in the Supporting Information.

Received: January 28, 2011
Revised: April 27, 2011
Published online: July 18, 2011

Keywords: bacteriorhodopsin · membrane proteins · NMR spectroscopy · protein structures

[1] J. P. Overington, B. Al-Lazikani, A. L. Hopkins, *Nat. Rev. Drug Discovery* **2006**, *5*, 993.
[2] H. M. Berman, J. Westbrook, Z. Feng, G. Gilliland, T. N. Bhat, H. Weissig, I. N. Shindyalov, P. E. Bourne, *Nucleic Acids Res.* **2000**, *28*, 235.
[3] S. H. White, *Nature* **2009**, *459*, 344.
[4] a) J. F. Wang, S. Kim, F. Kovacs, T. A. Cross, *Protein Sci.* **2001**, *10*, 2241; b) Y. Li, D. A. Berthold, R. B. Gennis, C. M. Rienstra, *Protein Sci.* **2008**, *17*, 199; c) I. Lehner, D. Basting, B. Meyer, W. Haase, T. Manolikas, C. Kaiser, M. Karas, C. Glaubitz, *J. Biol. Chem.* **2008**, *283*, 3281; d) V. Lange, J. Becker-Baldus, B. Kunert, B. J. van Rossum, F. Casagrande, A. Engel, Y. Roske, F. M. Scheffel, E. Schneider, H. Oschkinat, *ChemBiochem* **2010**, *11*, 547.

[5] a) O. C. Andronesi, S. Becker, K. Seidel, H. Heise, H. S. Young, M. Baldus, *J. Am. Chem. Soc.* **2005**, *127*, 12965; b) S. D. Cady, K. Schmidt-Rohr, J. Wang, C. S. Soto, W. F. DeGrado, M. Hong, *Nature* **2010**, *463*, 689.
[6] a) T. Hirai, S. Subramaniam, *FEBS Lett.* **2003**, *545*, 2; b) T. Hirai, S. Subramaniam, J. K. Lanyi, *Curr. Opin. Struct. Biol.* **2009**, *19*, 433.
[7] M. Etzkorn, S. Martell, O. C. Andronesi, K. Seidel, M. Engelhard, M. Baldus, *Angew. Chem.* **2007**, *119*, 463; *Angew. Chem. Int. Ed.* **2007**, *46*, 459.
[8] J. Yang, L. Aslimovska, C. Glaubitz, *J. Am. Chem. Soc.* **2011**, *133*, 4874.
[9] Y. Shen, F. Delaglio, G. Cornilescu, A. Bax, *J. Biomol. NMR* **2009**, *44*, 213.
[10] H. Patzelt, B. Simon, A. terLaak, B. Kessler, R. Kuhne, P. Schmieder, D. Oesterhelt, H. Oschkinat, *Proc. Natl. Acad. Sci. USA* **2002**, *99*, 9765.
[11] T. A. Cross, M. Sharma, M. Yi, H.-X. Zhou, *Trends Biochem. Sci.* **2011**, *36*, 117.
[12] C. G. Tate, G. F. X. Schertler, *Curr. Opin. Struct. Biol.* **2009**, *19*, 386.
[13] K. Varga, L. Aslimovska, A. Watts, *J. Biomol. NMR* **2008**, *41*, 1.
[14] K. Takegoshi, S. Nakamura, T. Terao, *Chem. Phys. Lett.* **2001**, *344*, 631.
[15] F. Castellani, B. J. van Rossum, A. Diehl, K. Rehbein, H. Oschkinat, *Biochemistry* **2003**, *42*, 11476.
[16] W. T. Franks, K. D. Kloepper, B. J. Wylie, C. M. Rienstra, *J. Biomol. NMR* **2007**, *39*, 107.
[17] F. Delaglio, S. Grzesiek, G. W. Vuister, G. Zhu, J. Pfeifer, A. Bax, *J. Biomol. NMR* **1995**, *6*, 277.
[18] W. F. Vranken, W. Boucher, T. J. Stevens, R. H. Fogh, A. Pajon, P. Llinas, E. L. Ulrich, J. L. Markley, J. Ionides, E. D. Laue, *Proteins Struct. Funct. Bioinf.* **2005**, *59*, 687.
[19] a) C. D. Schwieters, J. Kuszewski, N. Tjandra, G. M. Clore, *J. Magn. Reson.* **2003**, *160*, 65; b) C. D. Schwieters, J. J. Kuszewski, G. M. Clore, *Prog. Nucl. Magn. Reson. Spectrosc.* **2006**, *48*, 47.
[20] H. Belrhali, P. Nollert, A. Royant, C. Menzel, J. P. Rosenbusch, E. M. Landau, E. Pebay-Peyroula, *Structure* **1999**, *7*, 909.
[21] a) J. Kuszewski, A. M. Gronenborn, G. M. Clore, *Protein Sci.* **1996**, *5*, 1067; b) J. Kuszewski, A. M. Gronenborn, G. M. Clore, *J. Magn. Reson.* **1997**, *125*, 171.

